Influence of Polymer Side Chains on the Adjacent Microenvironment. A Fluorescence Probe Study by Means of Twisted Intramolecular Charge-Transfer Phenomena

Shigeo Tazuke,* Rong Kun Guo,[1] and Ryuichi Hayashi

Research Laboratory of Resources Utilization, Tokyo Institute of Technology, 4259 Nagatsuta, Midori-ku, Yokohama 227, Japan. *Received December 2, 1987; Revised Manuscript Received July 6, 1988*

ABSTRACT: Copolymers of ω-((4-(*N*,*N*-dimethylamino)benzoyl)oxy)dodecyl methacrylate were prepared using a large excess of an alkyl methacrylate where the alkyl group is methyl, butyl, cyclohexyl, or dodecyl. The content of the (dimethylamino)benzoate (DMAB) group, a fluorescence probe in the copolymer, is less than 0.04%. The dual-fluorescence spectra of polymer samples were studied in dilute solutions. The intensity ratio (R) of emission from the twisted intramolecular charge-transfer (TICT) state (a* band) to that from the planar non-CT excited state (b* band) provided useful information on the effect of a neighboring side chain on the twisting motion of the DMAB chromophore. The R value decreases with increasing bulkiness of the neighboring side chains. Excitation wavelength dependence of R indicates that there is a certain conformational distribution of DMAB already in the ground state. When the bulkiness of the neighboring side chain increases, the distribution becomes broader and the red-edge excitation effect on R becomes more prominent. These neighboring side chain effects on the twisting mobility of DMAB group are also dependent on polymer/solvent combinations.

Introduction

Recently, we reported a new method for obtaining detailed information on the segmental motion of polymer side chains in dilute solutions by means of twisted intramolecular charge-transfer (TICT) phenomena.[2-4] Our approach is based on the measurement of the TICT emission, reflecting the torsional motion of a part of the molecule and consequently the available free volume.[5,6] We used 4-(*N*,*N*-dimethylamino)benzoate (DMAB), a well-known TICT chromophore, as a fluorescence probe and linked the probe to poly(methyl methacrylate) (PMMA) via alkyl chains of variable length.[4] The ease of TICT state formation as determined by the intensity ratio (R) of emission from the TICT state (a* band) to that from the noncharge-transfer local excited state (b* band) is sensitively dependent on the distance between the probe and the main chain as well as on the solvent used.

Twisting motion of the TICT probe is released with increasing the spacer length between DMAB and the polymethacrylate main chain. Furthermore, the motion of the side chain terminal group is controlled more strongly by the polymer main chain in a poor solvent than in a good solvent. The structural effects on side chain mobility have not been studied systematically. Existing theories on polymer solution properties do not provide any interpretation on this subject.

If a polymer main chain with a fixed structure affects the motion of side chains depending upon their length, it is also likely that the motion of a side chain with a fixed length is affected in different ways by a neighboring side chain depending upon its length and bulkiness. In extending our previous works studying the length of spacer connecting the TICT probe to PMMA,[4] we examined the effects of surrounding side chains on the spectroscopic properties of the TICT chromophore bonded to the poly(alkyl methacrylate) main chain via dodecyl spacer. The present results together with the former ones provide information on the free volume distribution around a polymer main chain which might be otherwise difficult to be acquired.[7a] Such information will be useful for molecular engineering of speciality polymers, in particular those with active functions such as chemical reactivities, active transport in membrane, and so forth.

Scheme I

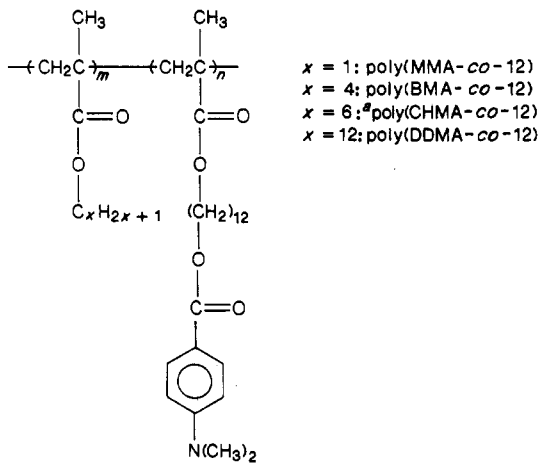

[a] For cyclohexyl, the number of hydrogen is $2x$.

Table I
Properties of Polymer Samples

polymer	M_n	chromophore content, wt %
poly(MMA-*co*-12)[a]	1.0×10^5	0.04
poly(BMA-*co*-12)	5.5×10^4	0.01
poly(CHMA-*co*-12)	5.0×10^4	0.02
poly(DDMA-*co*-12)	5.0×10^4	0.02

[a] The number of parentheses indicates the number of carbon atoms in the alkylene group connecting the TICT chromophore to the polymethacrylate.

Experimental Section

Materials. Poly(butyl methacrylate-*co*-12-((4-(*N*,*N*-dimethylamino)benzoyl)oxy)dodecyl methacrylate) (poly(BMA-*co*-12)), poly(cyclohexyl methacrylate-*co*-12-((4-(*N*,*N*-dimethylamino)benzoyl)oxy)dodecyl methacrylate) (poly(CHMA-*co*-12)), and poly(dodecyl methacrylate-*co*-12-((4-(*N*,*N*-dimethylamino)-benzoyl)oxy)dodecyl methacrylate) (poly(DDMA-*co*-12)) were prepared by the same method as poly(methyl methacrylate-*co*-12-((4-(N,*N*-dimethylamino)benzoyl)oxy)dodecyl methacrylate) (poly(MMA-*co*-12)) described in the previous publication.[4]

The abbreviations for the copolymers are based on the previous nomenclature. A general formula is given in Scheme I. The number-average molecular weights of the polymers were deter-

0024-9297/89/2222-0729$01.50/0

mined by gel permeation chromatography (HLC-802, Toyo Soda). The eluting solvent was chloroform, and our standard was a monodispersed polystyrene. The chromophore content was determined by UV absorption spectroscopy. Characterization of polymer samples is shown in Table I.

Solvents for spectroscopy were purified as follows. Butyl acetate (BuAc) was washed successively with 5% aqueous sodium carbonate and with saturated sodium chloride solution several times, dried over magnesium sulfate, and fractionally distilled over calcium hydride. Tetrahydrofuran (THF) was refluxed over $LiAlH_4$ and then distilled twice. 1,2-Dichloroethane (DCE) was washed with 5% sodium hydroxide solution and water and then fractionally distilled through an efficient column after drying over calcium chloride and phosphorus pentoxide. The purification of ethyl acetate (EAc) and butyl chloride (BuCl) was described previously.

Solvent–Polymer Interactions. Solubilities of the polymers were characterized by the second virial coefficient (A_2) determined by light scattering:[8]

$$K_c/R_\theta = M_w^{-1} + 2A_2C \quad (1)$$

R_θ and dn/dc were determined by a low-angle laser-light-scattering photometer (Chromatics KMX-6) and a differential refractometer (Union Giken RM-102), respectively. A_2 was obtained as the slope of the plot of K_c/R_θ versus C. The refractive index (n) was taken from the literature.

Spectroscopy. Fluorescence spectra were recorded under an argon atmosphere on a Hitachi MPF-4 spectrofluorometer. The spectroscopic data were corrected automatically for the instrumental response by an Oki IF-800 microcomputer. The relative emission intensity of the a* band to the b* band (R) was calculated by comparing the peak height of two emissions after correction. The spectral correction was made by separating two emissions. The correction for the overlapping of the b* band with the a* band was calculated by a PC-9801 computer (NEC). On the assumption that the shape of the a* band can be simulated by Gaussian distribution, the dual-fluorescence spectrum was reconstructed by the Simplex method[9] with six parameters, namely, peaking wavelength, height, and half-width for each band. Sample solutions for fluorescence spectroscopy were purged with argon for 30 min immediately before measurement. The polymer concentration was fixed at 1%. All measurements was carried out at room temperature.

Absorption spectra and fluorescence excitation spectra (corrected) were recorded on a Hitachi UV-320 spectrophotometer and a Hitachi F-4000 fluorescence spectrometer, respectively.

Results and Discussion

Effects of Neighboring Side Chains on Local Segment Motion. Figure 1 shows examples of the absorption and fluorescence spectra of poly(MMA-*co*-12), poly(BMA-*co*-12), poly(CHMA-*co*-12), poly(DDMA-*co*-12), and dodecyl 4-(*N*,*N*-dimethylamino)benzoate (DDDMAB) units as monomer model compounds in THF, BuCl, EAc, and BuAc. The excitation wavelength was fixed at 300 nm. Their absorption spectra are basically identical except for a slight broadening with an increase in size of the neighboring side chains.

Dual-fluorescence bands were observed in all cases. In comparison with the model compound, the intensity ratio (R) decreases in the polymers to different degrees depending upon their structure. Under the present experimental conditions, interchromophore interaction is negligible (DMAB content <0.04%), and the effect of polymer main chain, if any, should be very small and identical for all polymers since the DMAB chromophore is separated from the main chain via a dodecamethylene chain for all samples. Furthermore, dependence of the R value on polymer molecular weight is negligible.[4] Consequently, the large dependence of R value on polymer structure is attributable to the polymer side chain effects. Previously, Loutfy discussed a similar effect of polymer side chain on the maximum wavelength of fluorescence from a dye mixed

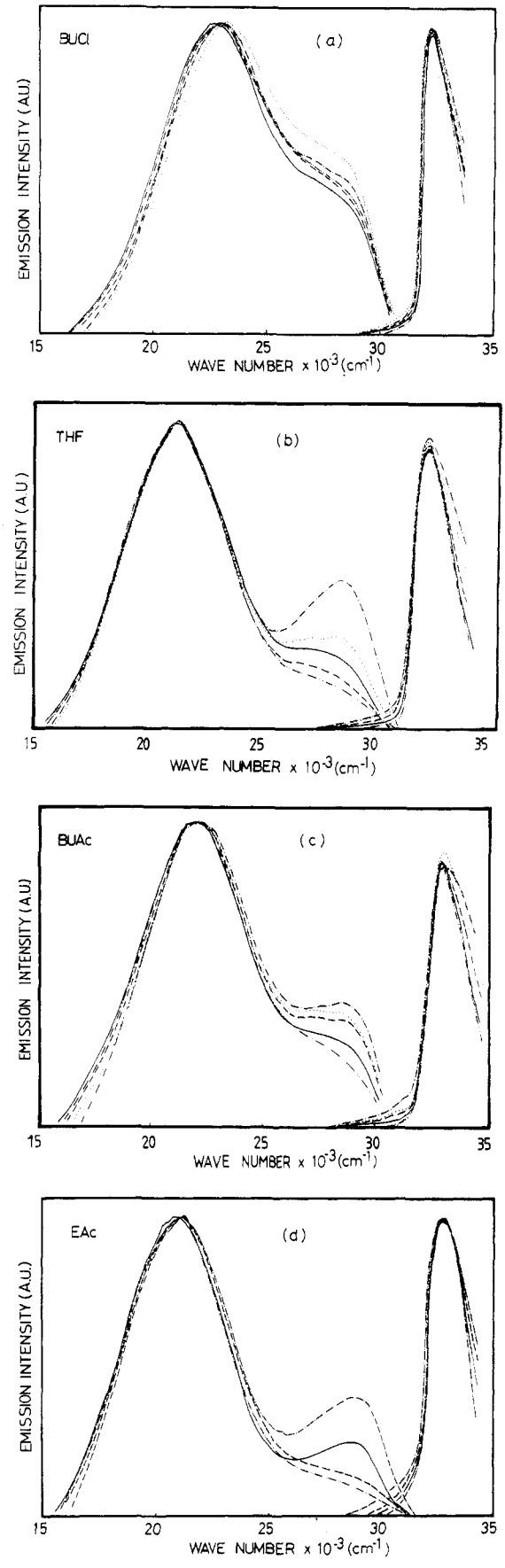

Figure 1. Absorption and fluorescence spectra of poly(MMA-*co*-12) (—), poly (BMA-*co*-12) (- - -), poly(CHMA-*co*-12) (- · -), poly(DDMA-*co*-12) (· · ·), and monomer model compound DDDMAB (- · · -) in BuCl (a), THF (b), BuAc (c), and EAc (d) at room temperature. Polymer concentration is 1 wt %. (DDDMAB) = 1×10^{-5} M. Excitation at 300 nm.

Table II
Solvent Effect on Second Virial Coefficient (A_2)[a] and the R Value of Various Polymers and the Monomer Model

		BuAc	EAc	BuCl	THF	DCE
solvent properties	ϵ	5.01 (20 °C)	6.01 (20 °C)	7.39 (20 °C)	7.58 (25 °C)	10.36 (25 °C)
	η	0.628 (30 °C)	0.400 (30 °C)	0.405 (30 °C)	0.460 (25 °C)	0.730 (30 °C)
poly(MMA-co-12)	10^2A_2	0.15	4.3	0.1	1.8	1.1
	R	4.73	5.38	2.95	5.03	3.59
poly(BMA-co-12)	10^2A_2	0.5	8.5	0.3	2.8	2.2
	R	5.35	9.26	3.32	6.00	5.05
poly(CHMA-co-12)	10^2A_2	0.3	0.2	0.15	3.2	1.2
	R	2.52	2.94	2.29	3.18	3.51
poly(DDMA-co-12)	10^2A_2	1.7		0.2	2.2	1.7
	R	3.85		1.89	3.63	3.33
DDDMAB	R	10.8	16.2	2.34	9.61	5.22

[a] See eq 1 in the text. [b] Poly(DDMA-co-12) is insoluble in EAc at room temperature.

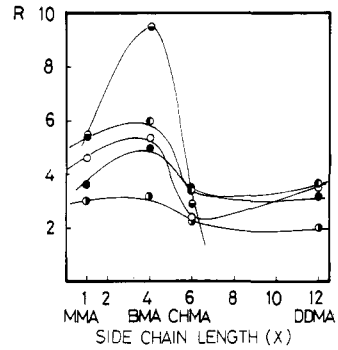

Figure 2. Emission intensity ratio (R) as a function of the carbon number (x) of neighboring side chain in BuAc (○), BuCl (◑), EAc (◒), THF (◐), and DCE (●). The conditions are the same as in Figure 1.

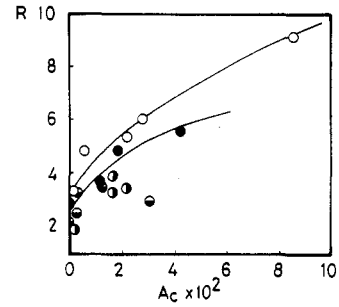

Figure 3. Relation between R and the second virial coefficient (A_2) of poly(MMA-co-12) (●), poly(BMA-co-12) (○), poly(CHMA-co-12) (◒), and poly(DDMA-co-12) (◑) in different solvents.

in a polymer matrix.[10] However, the probe is not of the dual-fluorescence type, so detailed information was not available. The structural effects depend on solvent as well, which will be discussed later.

Small but definite changes in the absorption spectra are also related to the restricted segmental motion depending upon the structure of neighboring side chains. If the TICT probe is no longer planar in the ground state owing to structural constraint, a shift in the absorption spectrum will result. The spectral shifts are relevant to the red-edge excitation effect.

The intensity ratio (R) as a function of carbon number (x) in the neighboring side chains is shown in Figure 2. A general tendency is for R to decrease with increasing size of the side chain. It is easily understandable that the bulkier neighboring side chains reduce local free volume in the vicinity and increase friction on rotational motion leading to the TICT state. However, there are some exceptions when the solvent is changed, revealing the importance of the polymer chain conformation. We determined the second virial coefficient (A_2) for the combination of four polymers with five solvents as shown in Table II. This allows us to discuss the relation between R and the size of the side chain together with the contribution of polymer–solvent interactions.

Poly(BMA-co-12) always has a larger R than poly(MMA-co-12) despite the longer alkyl side chain in the former. As shown by the larger A_2 in Table II, poly(BMA-co-12) exhibits better solubility than poly(MMA-co-12) in all solvents used. As we have discussed in a previous paper, side chain mobility is more strongly affected by the bulk of polymer chains in poor solvents than in good solvents. The anomalously large R of poly(BMA-co-12) is a result of an extended polymer chain where both main chain and side chain segments are rather thinly distributed around the TICT chromophore. Longer side chains restrict the twisting motion of the TICT group more, provided that the solubility parameters are identical. The present results indicate that the solubility of polymer is more important than the length of side chain.

However, poly(DDMA-co-12) exhibits a smaller R value than poly(MMA-co-12) and poly(BMA-co-12) in BuAc, in spite of its better solubility in the solvent. Obviously, when the alkyl side chain is very long, the neighboring side chain effect is enhanced irrespective of the degree of polymer–solvent interactions. In other words, the segmental motion at the end of a side chain is more sensitive to polymer conformation in the case of polymers bearing short side chains.

The relation between R and A_2 is presented in Figure 3. For poly(MMA-co-12) and poly(BMA-co-12), R increases distinctly with A_2, demonstrating the effect of polymer chain expansion. For the other two polymers, poly(CHMA-co-12) and poly(DDMA-co-12), the correlation of R with A_2 is not clear as for poly(MMA-co-12) and poly(BMA-co-12). The dependence of R on A_2 is much weaker for the polymers with longer or bulkier alkyl chains, revealing that the main chain conformation has less influence on side chain motion as the space occupied by the side chain is increased. Poly(CHMA-co-12), having a rigid cyclic side chain, exhibits a smaller R value in BuCl and THF than poly(DDMA-co-12), the polymer with the longest side groups, although the number of carbon atoms is CHMA is half of that in DDMA. Besides the effect of solubility, the rigidity of a side chain makes an important contribution to the side chain segment mobility at the neighboring positions. Stiffness of a series of cycloalkyl groups with five, six, seven, or eight-membered rings has been discussed on the basis of the dynamical mechanical behavior of poly(cycloalkyl methacrylate)s.[11] The cyclohexyl derivative was shown to have the least flexibility.

In the preceding discussion, we have assumed a priori that the formation of the twisted a* state from the planar b* state was one-way and dependent on the ease of the twisting molecular motion. According to Grabowski ki-

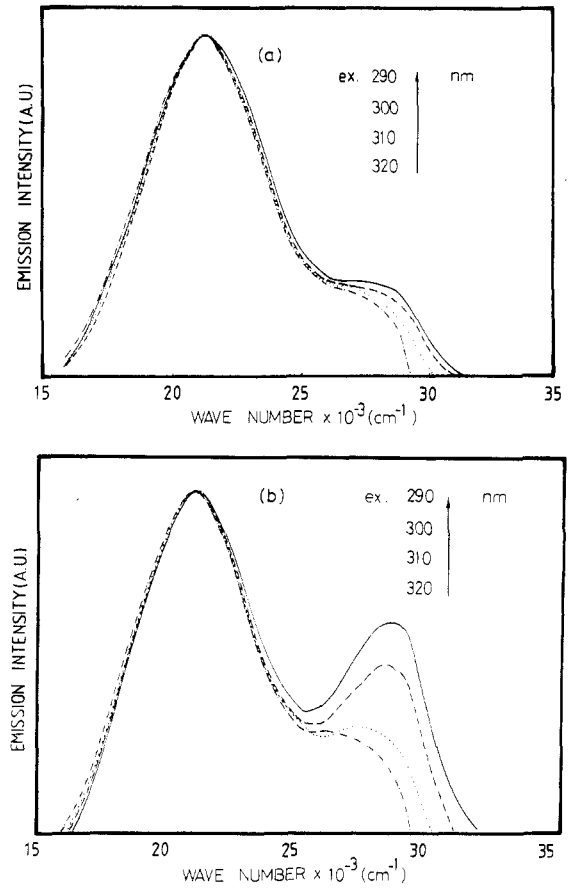

Figure 4. Excitation wavelength dependence of fluorescence from poly(MMA-*co*-12) (a) and poly(CHMA-*co*-12) (b) in 1 wt % THF solution.

netics,[6] interconversion between these two states could be either a nonreversible process or an equilibrium process depending upon temperature. The shape of the Arrhenius plot is similar to that observed for excimer formation.[12] When the temperature increases, the R value increases to a maximum and then decreases. The high-temperature region corresponds to the equilibrium region, and the lower temperature region involves an irreversible process. Most of the systems studied in this work belong to the high-temperature region or to the intermediate region close to the top of the bell-shaped Arrhenius plots at room temperature; that is, the equilibrium b* $\rightleftarrows$ a* is established.[13]

Measurements of temperature dependence of the R value revealed that the Arrhenius plots of all samples in THF, EAc, and BuAc did not intersect. Consequently, the sequence of R values at an arbitrary temperature represents the order at all temperatures and therefore the order of the rate constants for the b* $\rightarrow$ a* process to be determined in the low-temperature region.

Excitation Wavelength Dependence of *R*. The excitation wavelength dependence of TICT phenomena is an interesting subject.[14,15] When the conformational motion is slow relative to the excited state lifetime, a different set of conformers is excited with changing excitation wavelength. This phenomenon is called the red-edge effect (REE). Al-Hassan and Rettig have observed REE with several derivatives of *p*-(dimethylamino)-benzonitrile (DMABN) in a PMMA matrix.[16] We first observed REE for a polymer-bonded DMAB chromophore in dilute fluid solutions.[2] This shows that segmental motion in the polymer is retarded even in dilute solution. The magnitude is determined by the spacer length between the DMAB group and the main chain, indicating that the

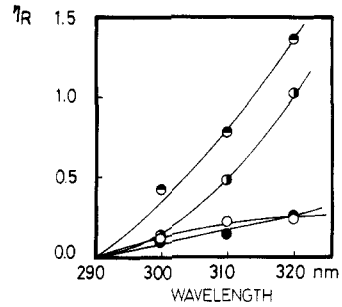

Figure 5. η_R as a function of excitation wavelength for poly(MMA-*co*-12) (●), poly(BMA-*co*-12) (○), poly(CHMA-*co*-12) (◓), and poly(DDMA-*co*-12) (◑) in THF.

ground-state conformation of the DMAB group is affected by the polymer chain.[4]

The REE is also dependent on the length and bulkiness of the neighboring side chain as shown in Figure 4. In the previous paper, we introduced the parameter η_R to evaluate the magnitude of REE for a polymer-bonded DMAB chromophore, where

$$\eta_R = (R_\lambda - R_{290})/R_{290} \qquad (2)$$

R_λ and R_{290} are the R values excited at λ nm and 290 nm, respectively. Here we adopted the same appraoch for evaluating the degree of REE. The relation between η_R and the excitation wavelength for the four copolymers in THF is given in Figure 5. The sequence of REE is as follows: poly(CHMA-*co*-12) > poly(DDMA-*co*-12) > poly(BMA-*co*-12) ~ poly(MMA-*co*-12). This sequence is similar in different solvents, although the magnitude is different.

Retting and co-workers have established the relation between the rate of TICT formation and the ground-state twist angle of the DMA group from the electron-accepting phenyl plane.[15,17] The presently observed REE is relevant to the different angular distribution of the DMA group in the ground state depending upon the size of neighboring side chains. The average twist angle of the DMA group will increase with increasing congestion so that the absorption band extends to a longer wavelength region. From a close look at Figure 1, we can recognize the broader absorption spectra of polymers with longer or bulkier side chains.

While the ground-state angular distribution decides the maximum degree of REE, the actual magnitude should depend on molecular dynamics. REE will be most pronounced when twisting to the a* state from the already twisted ground state is fast enough and that from the planar ground state is slow in comparison with the lifetime of the a* state. This is possibly the case for poly(CHMA-*co*-12) bearing bulky cyclic side chains.

The monitoring wavelength dependence of excitation spectra in Figure 6 supports the above discussion. When the monitoring wavelength is changed from the b* band (350 nm) to the a* band (430 nm), the excitation spectra shift to red. This shift is larger for poly(CHMA-*co*-12) than for poly(MMA-*co*-12), indicating that the excitation of a somewhat twisted ground state absorbing at longer wavelength is particularly favored for the formation of the TICT state in poly(CHMA-*co*-12). The excitation spectra of the other polymers fall in between these two.

In addition to the gain in a* band intensity with the excitation at 320 nm, the b* band shifts slightly to the red as compared with the fluorescence excited at 290 nm for polymer samples (Figure 4). This is understandable if the partially twisted b* state does not relax to the planar b* state during its lifetime.

Table III
Neighboring Side Chain Effects on TICT Phenomena

side chain	steric effect	intensity ratio $R = I_{a^*}/I_{b^*}$	absorption spectra	red-edge excitation effect (REE)	dependence of R on A_2
CH_3 C_4H_9 $C_{12}H_{25}$ cyclohexyl	↓ increases	↑ decreases	↓ broadened	↓ enhanced	↓ obscured
	bulkiness and/or stiffness of the side chain increases	rates of b* → a* are reduced	distribution of twisted ground-state conformation becomes broader and the probability of TICT state formation is reduced		importance of main chain conformation is reduced

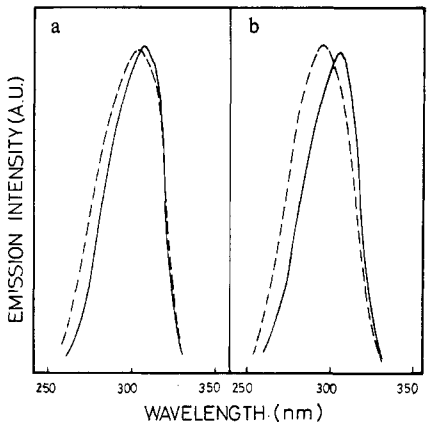

Figure 6. Fluorescence excitation spectra of poly(MMA-*co*-12) (a, left) and poly(CHMA-*co*-12) (b, right) in EAc. (—) Monitored at the a* band (430 nm), (---) monitored at the b* band (350 nm).

Specificity of Solvent Effects on TICT Phenomena. The position of the a* band provides information on the local polarity in the vicinity of TICT chromophore since the polar a* is more stabilized by solvation.[5,6] The emission maximum, $\nu_{max}(a^*)$, as a function of the side chain carbon number, x, is shown in Figure 7.

In THF and BuAc, $\nu_{max}(a^*)$ remains almost constant for all polymers and the monomer model compound. Although the molecular motion depends on the polymer structure, the TICT chromophore is equally exposed to solvent independent of polymer structure, and the difference in properties between the polymer chain and these solvents is not large enough to cause a large spectral shift. In particular, the polymer chain effect is reduced in good solvents. Generally speaking, the polymer chain reduces solvation of a polar excited state such as the TICT state or exciplex, causing the emission maximum to shift to a higher energy in comparison with the relevant monomer model systems.[18] This trend is observed vaguely only in EAc. A small blue shift is observed in EAc when the alkyl side chain is extended. This solvent is a poor solvent for polymethacrylates with long alkyl side chains, and consequently, the nonpolar nature of the side chain is more strongly reflected in the energy level of the a* state than in THF or BuAc.

In addition to the static solvent effects, as shown by the time-dependent red shift of polymer-bonded exciplex,[19] the relaxation rate for the formation of the solvent-equilibrated excited state is slower in the polymer. In poor solvents, the retardation of solvation will be more important. This situation will cause a further blue shift in emission in polymeric systems. The general trend found in a polymer is that polarity in a polymer microenvironment is lower than the solvent polarity particularly in polar poor solvents. Studies on solvatochromic shifts of dyes in polymers[20,21] and solvent effects on polymer-bonded exciplexes[22,23] led to the conclusion that solvent polarity is less effective in polymeric systems.

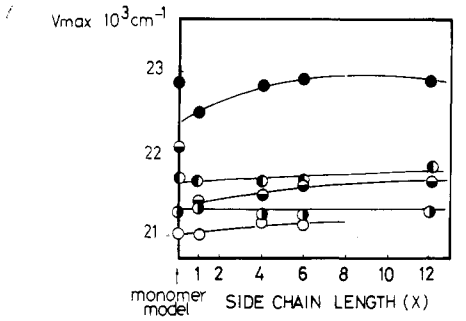

Figure 7. Maximum emission frequency (V_{max}) of the a* band as a function of the carbon number of neighboring side chain in BuCl (●), EAc (○), BuAc (◐), DCE (◒), and THF (◐).

The behavior of halogenated solvents is also abnormal for both $\nu_{max}(a^*)$ (Figure 7) and the R value (Figure 1). The a* emission of the monomer model appears at an unexpectedly deeper blue region in halogenated solvents in comparison with the value observed in other solvents of comparable polarity. There seems to be specific solvent–TICT compound interaction, but the details are not clear. In other solvents, R values for polymers are smaller than for the monomer model, reflecting reduced molecular motion. In BuCl and DCE, R values for the monomer model are unusually low, and even lower than the values for polymers in BuCl. This is not because of differences in viscosity of polarity, since the physical constants in Table II are quite comparable for all solvents. This apparently abnormal behavior is attributable to different trends in the bell-shaped Arrhenius plots for the monomer model and the polymers in these solvents. In polymer systems, the temperature giving the maximum R value (T_{max}) shifts toward higher temperature, indicating that the contribution of the b* ← a* reverse process is impeded. The present measurements were conducted slightly above T_{max} of the polymers, whereas the T_{max} for the monomer model is very much lower. Consequently, the reverse process contributes significantly only in the monomer model system where the R value is very low. If we compare the R value at lower temperature where the reverse process can be neglected both for the polymers and the monomer model, the sequence of the R value is normal.

Conclusion

Polymer side chain effects on the TICT emission behavior are summarized in Table III. In brief, these effects consists of three factors. First, polymer side chains control the ground-state conformational distribution of the DMAB chromophore as demonstrated by the REE and the broadening of the absorption spectra. Second, the R value suggests the retardation of TICT state formation depending upon the neighboring alkyl side chains. Finally, the polymer chain conformation is an important factor controlling side chain mobility, in particular when the side chain is short. All these factors are closely related to the

degree of polymer chain expansion as well as the length and bulkiness of side groups.

The qualitative data presented in this article will be elaborated on in a more quantitative manner by means of time-resolved fluorescence spectroscopy determining directly the rate of molecular motion.

Acknowledgment. The authors are greatly indebted to Professor M. Sisido and Dr. N. Kitamura for their valuable discussions.

Registry No. (BMA)(12) (copolymer), 116911-34-3; (CHMA)(12) (copolymer), 116911-35-4; (DDMA)(12) (copolymer), 116911-36-5; (MMA)(12) (copolymer), 112925-63-0; DDDMAB, 77016-80-9.

References and Notes

(1) Visiting fellow from Institute of Photographic Chemistry, Academia Sinica, Beijing, China.
(2) Hayashi, R.; Tazuke, S.; Frank, C. W. *Macromolecules* **1987**, *20*, 983.
(3) Hayashi, R.; Tazuke, S.; Frank, C. W. *Chem. Phys. Lett.* **1987**, *135*, 123.
(4) Tazuke, S.; Guo, R. K.; Hayashi, R. *Macromolecules* **1988**, *21*, 1046.
(5) Rettig, W. *Angew. Chem., Int. Ed. Engl.* **1986**, *25*, 971.
(6) Grabowski, Z. R.; Rotkiewicz, K.; Rubaszewska, W.; Kirbarkamirska, E. *Acta Phys. Pol., A* **1978**, *A54*, 767.
(7) (a) Hoyle, C. E. *Photophysics of Polymers*; ACS Symposium Series; Hoyle, C. E., Torkelson, J. M., Eds.; American Chemical Society: Washington, DC, 1987; p 4. (b) Hayashi, R.; Tazuke, S.; Frank, C. W. *Ibid.* p 135.
(8) *Polymer Handbook*, 2nd ed.; Branddrup, J., Immergut, E. H., Eds.; Wiley Interscience: New York, 1970. M_w, weight-averaged molecular weight; C, polymer concentration in g/mL; R_θ, reduced Rayleigh factor; K, optical constant given by $K = 4.079 \times 10^6 n^2 (dn/dc)^2$ where n is the refractive index of solvent. dn/dc is the dependence of n on concentration. See the instruction manual for KMX-6 low-angle light-scattering photometer.
(9) Nelder, J. A.; Mead, R. *Comput. J.* **1963**, *6*, 163.
(10) Loutfy, R. O. *Photophysical and Photochemical Tools in Polymer Science*; Winnik, M. A., Ed.; D. Reidel: Dordrecht, 1986; p 429.
(11) Heijboer, J. *J. Polym. Sci., C* **1968**, *16*, 3413.
(12) Birks, J. B. *Photophysics of Aromatic Molecules*; Wiley Interscience: New York, 1970; Chapter 7.
(13) The TICT state formation is irreversible for poly(CHMA-*co*-12) in BuCl and THF and for poly(MMA-*co*-12) in BuCl at room temperature. Namely, these three systems are in the low-temperature region at room temperature, and the b* and a* states are not equilibrated. The shapes of the Arrhenius plots depend on solvent very much. Apparently, the rates and activation parameters of both forward and reverse processes are solvent dependent, for which we have no satisfactory interpretation at the moment. Temperature dependence of R values as functions of polymer structure and solvent is the subject for separate publications. See discussion in the final section.
(14) Al-Hassan, K. A.; El-Bayoumi, M. A. *Chem. Phys. Lett.* **1980**, *76*, 121.
(15) Rettig, W. *J. Luminesc.* **1980**, *26*, 21.
(16) Al-Hassan, K. A.; Rettig, W. *Chem. Phys. Lett.* **1986**, *126*, 273.
(17) Lippert, E.; Rettig, W. *Adv. Chem. Phys.* **1987**, *67*, and many references therein.
(18) (a) Tazuke, S.; Yuan, H. L. *Polym. J.* **1982**, *14*, 215. (b) Yuan, H. L.; Tazuke, S. *Polym. J.* **1983**, *15*, 111.
(19) Tazuke, S.; Higuchi, Y.; Tamai, No.; Kitamura, N.; Tamai, Na.; Yamazaki, I. *Macromolecules* **1986**, *19*, 603.
(20) (a) Strop, P.; Mikes, F.; Kalal, J. *J. Phys. Chem.* **1976**, *80*, 694; (b) *Macromolecules*, **1973**, *13*, 345.
(21) Mikes, F.; Strop, P.; Kalal, J. *Makromol. Chem.* **1974**, *175*, 2375.
(22) Tazuke, S.; Matsuyama, Y. *Macromolecules* **1977**, *10*, 215.
(23) Tazuke, S.; Iwaya, Y.; Hayashi, R. *Photochem. Photobiol.* **1982**, *35*, 621.

Association of Hydrophobic Polymers in Water: Fluorescence Studies with Labeled (Hydroxypropyl)celluloses

Françoise M. Winnik

Xerox Research Center of Canada, 2660 Speakman Drive, Mississauga, Ontario L5K 2L1, Canada. *Received April 26, 1988; Revised Manuscript Received July 19, 1988*

ABSTRACT: The occurrence in water of interpolymeric association between fluorescently labeled (hydroxypropyl)cellulose was demonstrated on the basis of nonradiative energy transfer between chromophores attached to different polymer chains. The two polymers were a pyrene-labeled (hydroxypropyl)cellulose (HPC-Py/438) containing on average 0.5 pyrene per chain and a fluorene-labeled (hydroxypropyl)cellulose (HPC-Flu/33) containing on average three fluorene groups per chain. Energy transfer between fluorene, the energy donor, and pyrene, the energy acceptor, was detected in aqueous solutions of HPC-Py/438 and HPC-Flu/33 for total polymer concentrations as low as 0.02 g L^{-1}. No energy transfer occurred between the labels when the two polymers were dissolved in methanol or dioxane. The steady-state and time-dependent fluorescence spectroscopy of HPC-Flu/33 is described. In water, methanol, and dioxane the polymer exhibited an emission of intensity I_M centered at 317 nm due to isolated excited fluorenes and an emission of intensity I_E centered at 395 nm due to fluorene excimers. In a given solvent the ratio I_E/I_M remained constant over the concentration range of 0.01 to 0.1 g L^{-1}. The ratio was larger for polymer solutions in water (0.49) than in dioxane (0.14).

Introduction

The architecture of organized systems in water reflects a delicate balance of forces. Coulombic forces, ion pair formation, hydrogen bonding, and hydrophobic interactions all contribute to the stability of self-assembling natural systems, such as micelles, vesicles, or membranes. Synthetic polymers also form organized assemblies. These provide attractive options for the design of functional devices. Tools for the study of microdomains in solutions are numerous.[1] They yield information on parameters such as the size and distribution of the microdomains, their electric charge, or their hydrophobicity. The experiments described here use fluorescence techniques to study aggregates of an industrially important polymer, (hydroxypropyl)cellulose (HPC). This polymer is an additive in many commercial materials, such as paints, inks, cosmetics, pharmaceuticals, foods, ceramics, and coatings.[2] It is a water-soluble polymer prepared from cellulose by attachment of hydroxypropyl ether groups to the glucose hydroxyl substituents. Minor chemical modifications of the polymer structure can alter dramatically the solution properties of cellulose ethers. An intriguing example is that

0024-9297/89/2222-0734$01.50/0